Supplementary Material

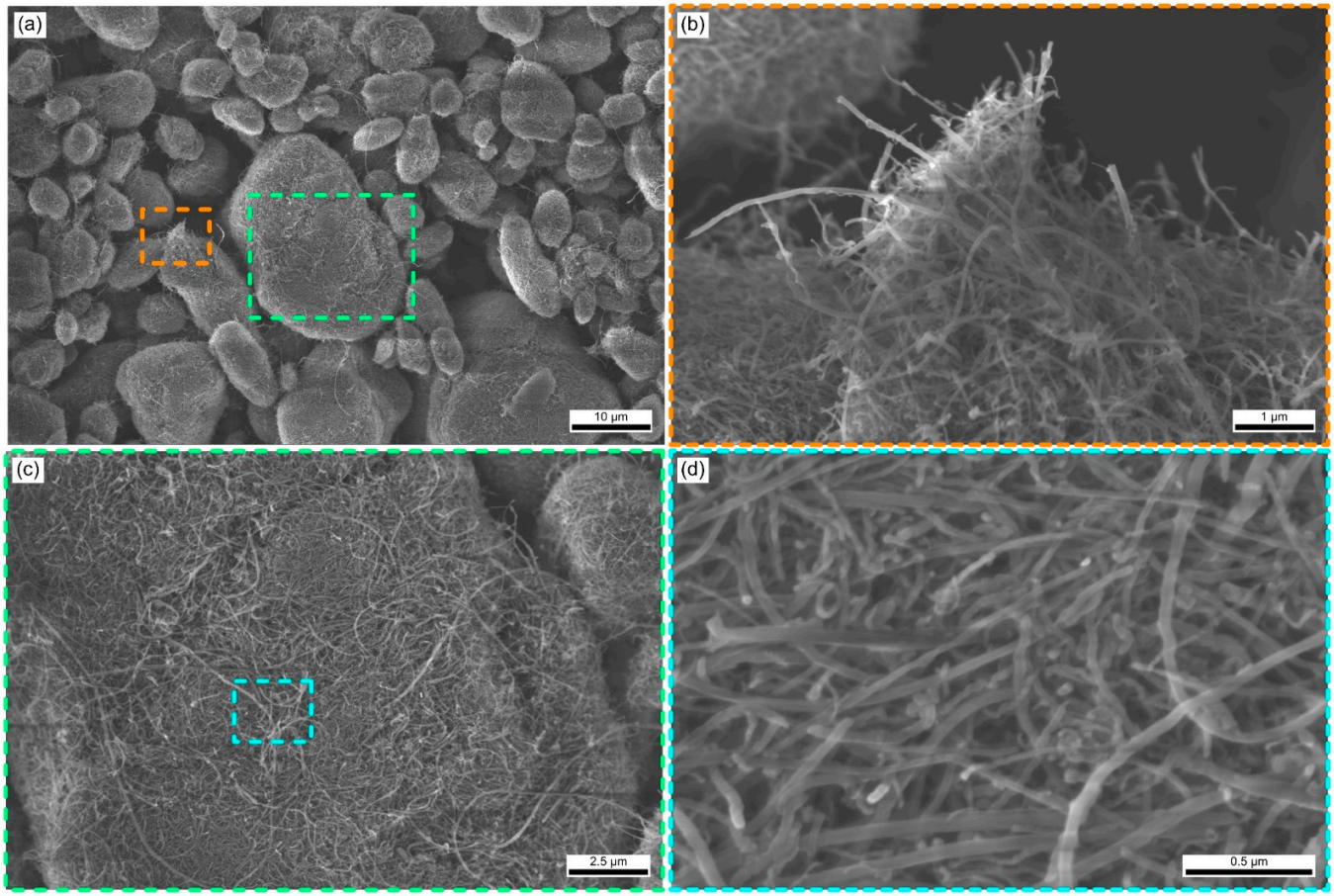

Figure S1. SEM micrographs of pristine CNT at different magnifications.

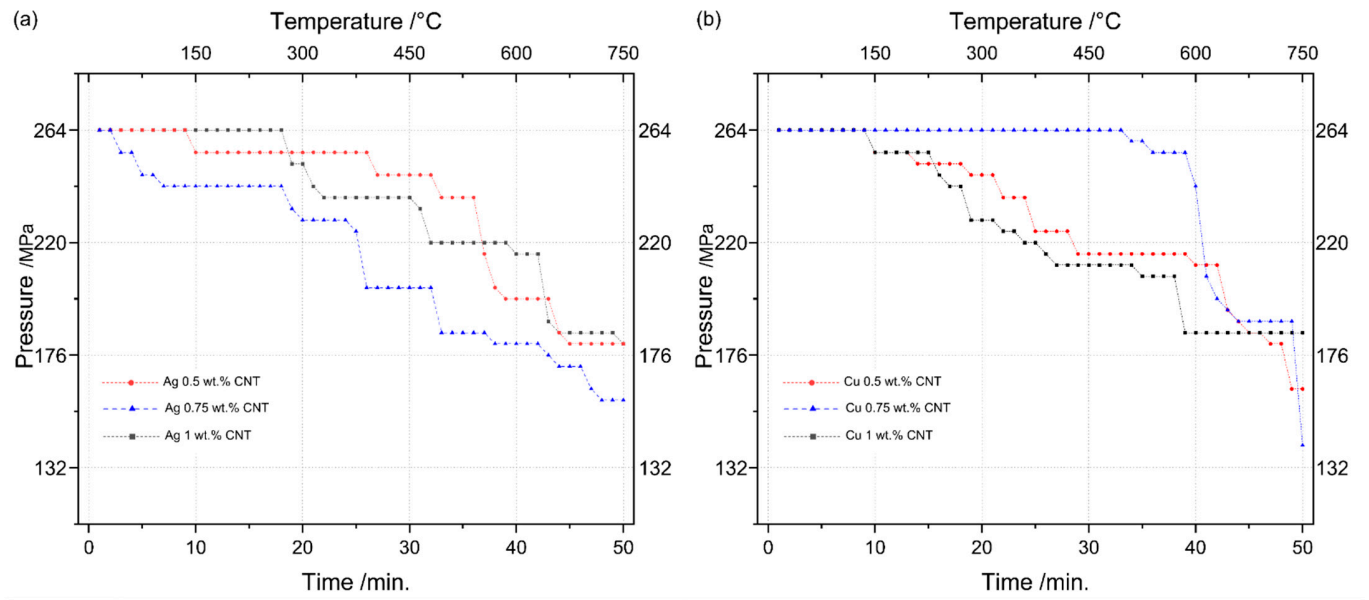

Figure S2. Pressure variation during heating stage of HUP for (a) Ag-MMC and (b) Cu-MMC.

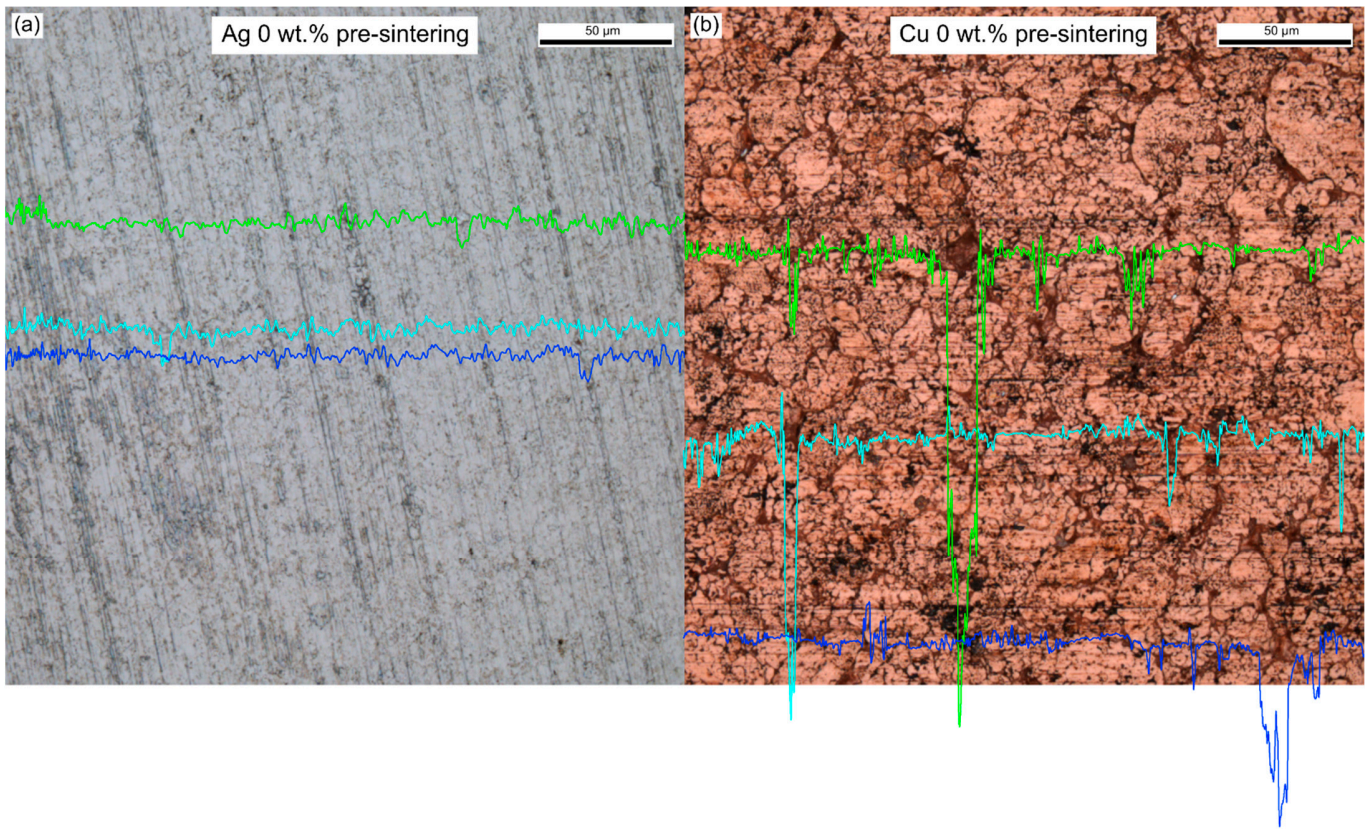

Figure S3. 50× surface CLSM scan of green pellets (pre-sintered samples) showing three linear roughness scans in regions with open porosities.

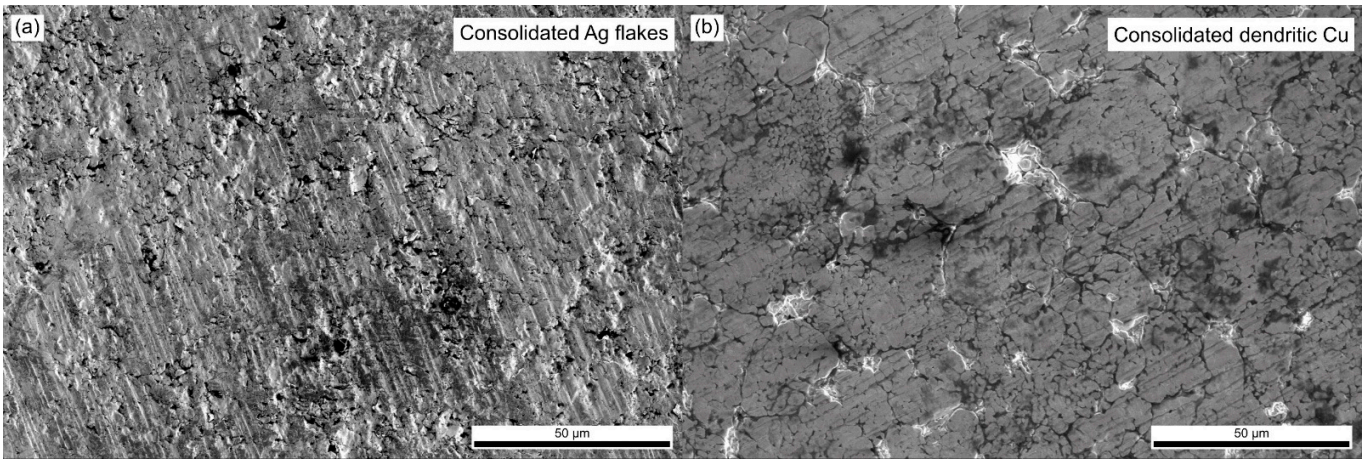

Figure S4. Surface SEM micrograph of consolidated a) silver flakes and b) dendritic copper powder.

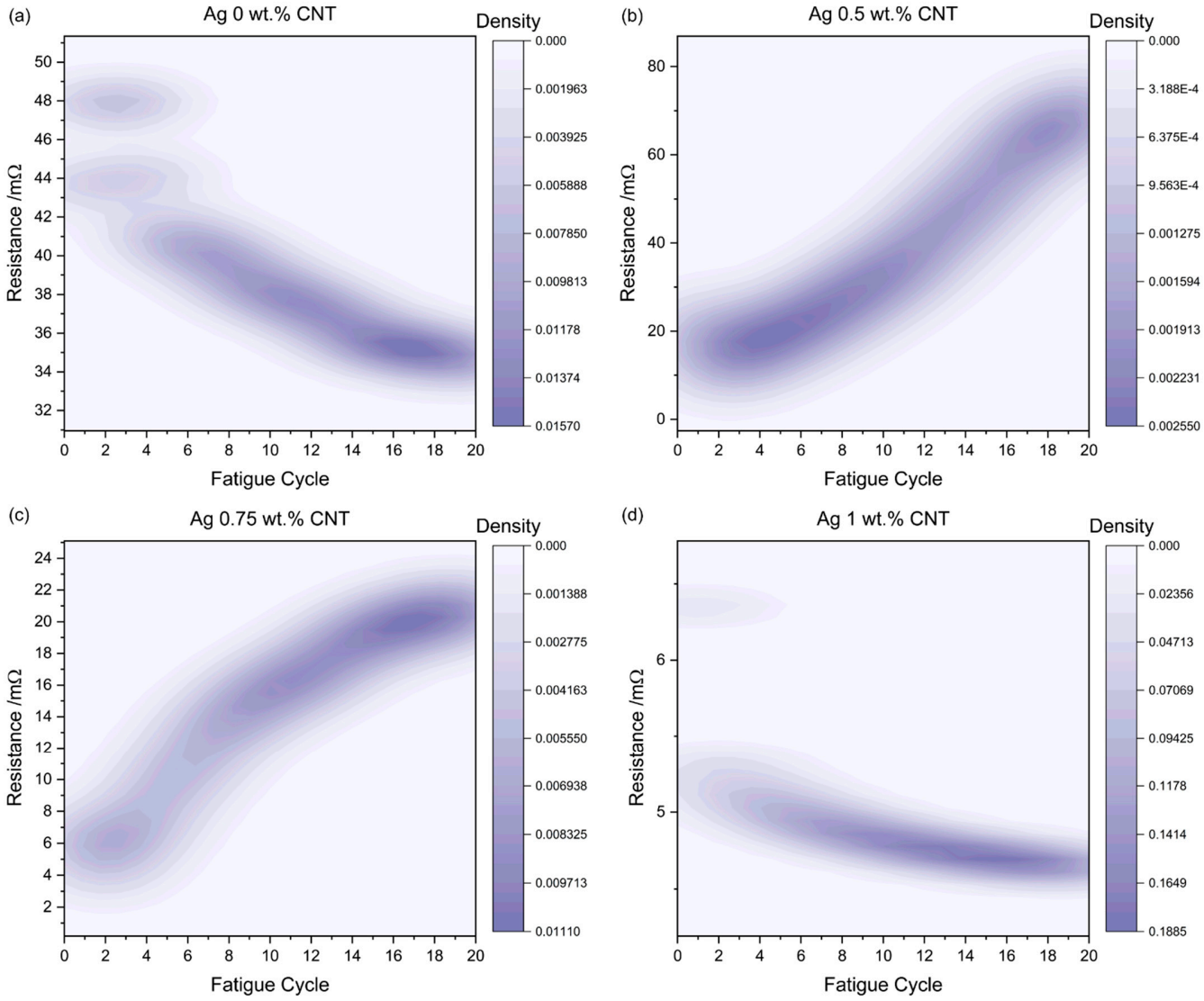

Figure S5. Kernel density estimation plot of ECR during multiple fatigue cycles of CNT reinforced Ag matrices. (a) Ag 0%, (b) Ag 0.5%, (c) Ag 0.75%, and (d) Ag 1%. Note the different y-axis ranges.

Table S1. Roughness values prior to and post-fatigue tests of silver MMC, as well as approximate imprint diameter left by counter electrode.

	Roughness prior to fatigue tests/nm	**Roughness post-fatigue tests/nm**	**Imprint diameter/μm**
Ag 0%	10 ± 10	30 ± 10	58.4 ± 5.2
Ag 0.5%	20 ± 10	80 ± 10	74.8 ± 8.7
Ag 0.75%	40 ± 10	120 ± 30	87.5 ± 2.5
Ag 1%	60 ± 10	100 ± 10	76.3 ± 2.7

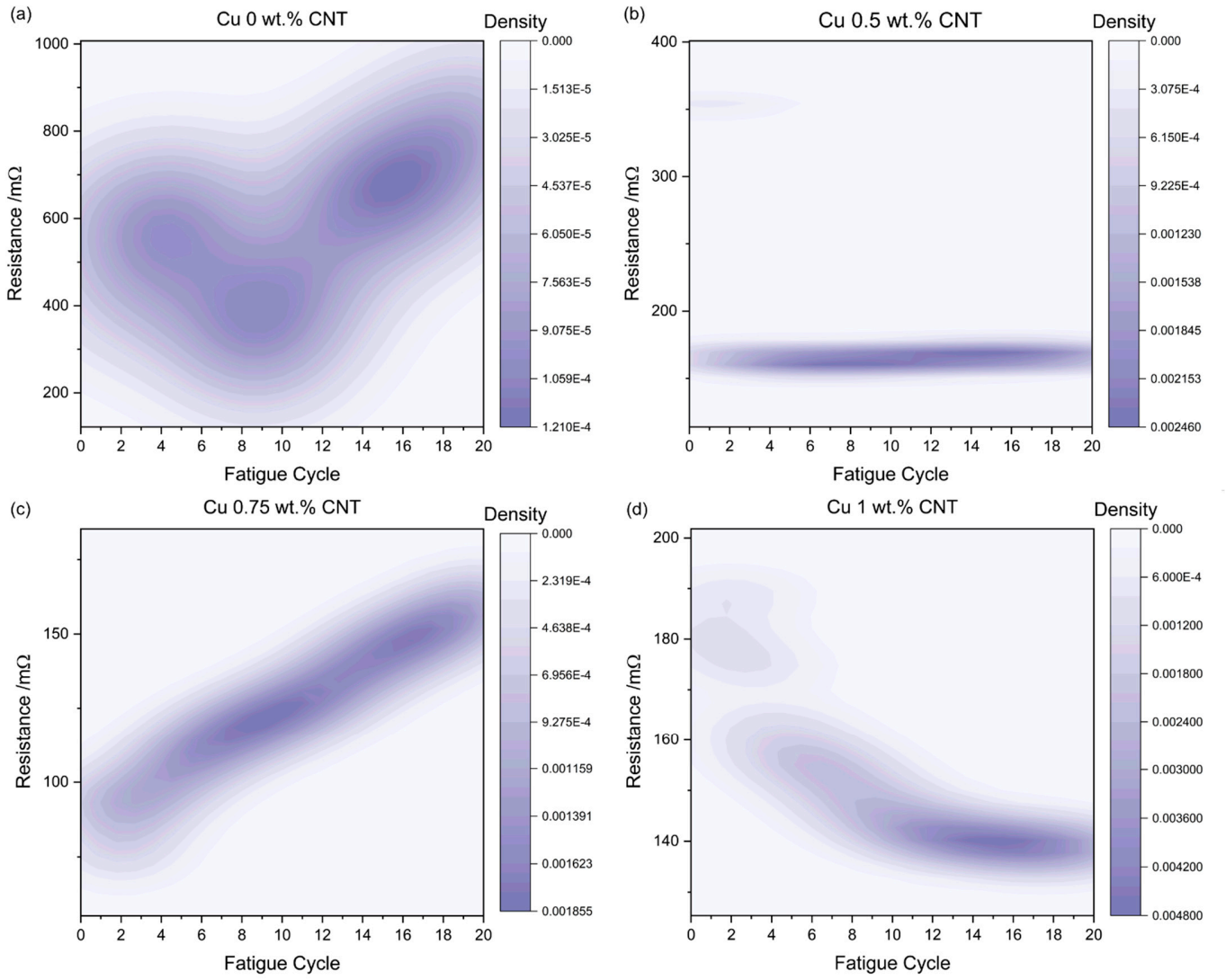

Figure S6. Kernel density estimation plot of ECR during multiple fatigue cycles of CNT reinforced Cu matrices. (a) Cu 0%, (b) Cu 0.5%, (c) Cu 0.75%, and (d) Cu 1%. Note the different y-axis ranges.

Table S2. Roughness values prior to and post-fatigue tests of copper MMC, as well as approximate imprint diameter left by counter electrode.

	Roughness prior to fatigue tests/nm	**Roughness post-fatigue tests/nm**	**Imprint diameter/μm**
Cu 0.5%	70 ± 10	220 ± 90	58.5 ± 3.5
Cu 0.75%	90 ± 10	150 ± 20	76.0 ± 1.6
Cu 1%	80 ± 10	130 ± 30	60.1 ± 3.2

* Cu 0% could not be measured. The imprint of the counter electrode could not be observed due to the higher hardness of the reference sample.